131
71

Axial Strain Effects On Optical Fiber Mode Patterns

by

K.T.Srinivas

Thesis submitted to the Faculty of the

Virginia Polytechnic Institute and State University

in partial fulfillment of the requirements for the degree of

Master of Science

in

Electrical Engineering

APPROVED:

Richard O. Claus

R. O. Claus, Chairman

R. J. Pieper

R. J. Pieper

Poon Jing Chung

T. C. Poon

January 1987

Blacksburg, Virginia

Axial Strain Effects On Optical Fiber Mode Patterns

by

K.T.Srinivas

R. O. Claus, Chairman

Electrical Engineering

(ABSTRACT)

Axial strain effects in multimode fibers are studied. A few-mode fiber is mounted on a tensile testing machine and strained at various speeds. The output of a monochromatic light source passing through it is monitored and recorded. Relations are noted between the light output the magnitude of tension and the rate of the applied axial strain. Flexural behaviour of the optical fiber at various tensions is also studied by monitoring the modal output pattern. Relations are compiled to serve as a beginning to model these and other related modal effects. A theoretical background is also suggested to explain the observed effects.

Acknowledgements

I would like to express my sincere appreciation to my advisor, Dr. Richard. O. Claus, for his ideas and guidance, and in particular, his endless enthusiasm. I am particularly grateful to him for having introduced me to the fascinating field of Ftber Optic Sensors. I also wish to thank the other members of my advisory committee, Dr. T.C. Poon and Dr. R.J. Pieper, for their comments, suggestions and encouragement.

I am also grateful to the members of the fiber optic group, Kim D Bennet, N K Shankar, Paul Ehrenfeuchter, Kent Murphy and Mahesh Reddy for their suggestions and help on this project. I would also like to thank Ms. Robin Rogers and Ms. Ann Goette for willing to share their time and helping me with the drawings and figures.

Table of Contents

1.0 Introduction 1

1.1 Motivations and Overview 5

1.2 Fundamentals of Optical Transmission in Fibers 7

1.3 Polarimetric Sensing 8

1.4 Introduction to 'Modal Domain' Sensing 8

2.0 Theoretical Background 10

2.1 Introduction to Stress and Strain in Solids 10

2.1.1 Stress 10

2.1.2 Strain 14

2.1.3 Relation Between Stress and Strain 16

2.2 Optics of Photoelasticity 17

3.0 Mechanisms of Modulation 19

3.1 Phase modulation mechanisms in fibers 19

3.2 Mechanisms of Polarization Modulation 24

4.0 Experiment and Observations **29**

4.1 Motivation and Reasons 29

4.2 Apparatus 30

4.3 Experiment and Observations 31

5.0 Conclusions **37**

5.1 Discussion 37

5.2 Conclusion 39

5.3 Suggestions 39

6.0 References **41**

VITA **43**

List of Illustrations

Figure 1. Basic fiber-optic interferometer 4
Figure 2. Components of force and stress 11
Figure 3. Displacement of line elements 12
Figure 4. Stress components in rectangular co-ordinates 15
Figure 5. Experimental set-up. 33
Figure 6. Output for 0.5 mm/min displacement rate. 34
Figure 7. Output for 1.0 mm/min displacement rate. 34
Figure 8. Output as tension is applied. 35
Figure 9. Output as tension is released. 35
Figure 10. Output due to vibrating beam at the two states of tension. 36

1.0 Introduction

The potential of optical fibers as passive non-intrusive sensors of a wide range of physical observables has been well recognized and exploited for more than ten years. The main advantages of optical fibers for sensor applications are their intrinsic dielectric nature, geometric flexibility and small size, providing considerable design versatility particularly suited for certain remote sensing applications.

The development of optical fiber sensors began in 1977 with the development of optical fiber acoustic sensors [1] The following few paragraphs describe some of the past and more recent applications of optical fibers as sensors.

The operation of all-fiber optic sensors is based upon the modulation of the propagation parameters of light which travels through the fibers. These parameters are intensity, phase, polarization, wavelength and mode.

Intensity modulation is the simplest sensing mechanism to implement. The usual measurand is the relative displacement one or two parts attached to the fiber. The sensor is configured as a microbend transducer, either a reflection type or simple butt coupling type [2]. Of these the microbend sensor

is the most sensitive with resolution of fractions of Angstroms. In general this variety of sensors has a dynamic range of 50-70 dB [2].

By comparision, optical phase modulators have a remarkable sensitivity. Dynamic ranges of 10^7 are quite easily obtained even for quasi static measurements. These are used in the form of interferometers in most cases. It should be noted that other kinds of modulations also manifest themselves as some form of phase modulation. The most useful application of these devices is the monitoring of temperature, pressure and strains.

Polarization is potentially another powerful modulation mechanism. In most polarization-based devices the fiber itself is the sensor. Monomode fibers are used in most cases and depend on the ability of the measurand to alter the polarization state of the light propagating through the fiber. The principal application has been in the sensing of large electric currents.

Wavelength based sensors are usually in the form of color probes. Here the fiber simply serves to feed light from a source to the monitoring region and to return the modulated light for analysis. Usually large core, high NA fiber is used.

The effect of mechanical perturbations on the various modes propagating in a multimode fiber is yet another method of exploiting the usefulness of fibers as sensors. This a relatively new area of research and applications of this method include the monitoring of vibrations, acoustic emission, etc. [3,4].

Given below are some of the specific applications of fibers as sensors which have been available for the past few years. [1]

Acoustic Sensors

Most work in this area was conducted at the Naval Research Laboratories for underwater acoustic detection via hydrophones in the late 1970's. These generally employ the two arm phase modulated

Mach-Zehnder interferometer or the single fiber, polarimetric type. The former consists of a reference arm and a sensing arm (see Figure 1).

In the reference arm some means is provided to either shift the optical frequency or for phase modulation. The two beams are usually recombined on the surface of a photodetector and suitably demodulated. Modulation of light in the fibers is dependent upon the frequency and amplitude of the impressed acoustic signal. Alternatively, such sensors may be configured as a gradient type in which both arms of the interferometer encounter the signal. Here what is sensed is the gradient and the direction of a pressure wave. In the polarimetric version of this sensor, a single mode fiber has the polarization states of its cross polarized components modulated due to differential birefringence effects produced by the ultrasonic signals. In these applications the fiber is generally configured as a coil. Varying the winding density of such coil structures allows us configure arrays of such sensors.

Magnetic Sensors The measurement of magnetic fields is based on principally two effects; the Faraday effect and the magnetostrictive effect. The former requires special kinds of fibers to be able to be sufficiently sensitive. Sensitivities of $10^{-4}G/m$ seem possible in rare earth doped optical fibers. Most magnetic sensors generally work on the second principle as it is more sensitve and does not require the use of any specially doped fiber. Here the fiber is placed in close contact with a magnetostrictive material which changes physical dimension in the presence of a magnetic field. This causes a proportional strain in the attached fiber which results in an optical phase change in an interferometric set-up. The key research in this application is in identifying appropriate magnetostrictive materials to be bonded or coated on to the fibers. Magnetic fields from $10^{-5} - 10^{-9}$G/m are predicted to be detectable by this method [1].

Fiber Optic Gyros Passive ring interfrometers have shown promise as inertial rotation sensors . Here a single mode fiber is arranged in a ring to form a Sagnac interferometer. Two counterpropagating beams of light are injected into the rotating fiber loop which causes a phase difference between them. When these two beams are recombined on a detetctor we get a rotation dependent intensity modulation of the light. Sensitivities of as small as 1 deg/hr have been announced.

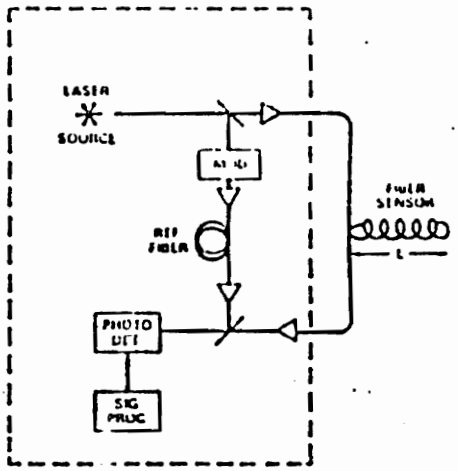

Basic fiber optic interferometer.

Figure 1.

Several other kinds of amplitude sensors are also available[1]. These include microbend type sensors, displacement type sensors and others. The former is based on the principle that a fiber subjected to a spatially periodic bending causes coupling between modes having a propagation constant difference which is proportional to this periodicity. This kind of transducer has been assembled both as a strain and as a dynamic acoustic sensor . Displacement sensors include reflection types that depend upon the movement of a reflecting surface to modulate light being coupled into an adjacent fiber, and the simpler position dependent variety which alters the coupling between two fibers butted together but free to move independently.

1.1 Motivations and Overview

A particularly attractive application of optical fiber sensors is for the monitoring of stress and strain because they have the potential of offering a highly competitive method of nondestructive evaluation in certain hostile or harsh environments. Related applications include the measurement of pressure, temperature, acoustic emission in materials as well as the vibrational modes of strings, beams and similar structures [3]. All these perturbations affect the transmission of light through physically straining the fiber. As a strain sensor, optical fiber is robust. Although the fiber is made of glass its very high elastic modulus makes it remarkably resilient to damage.

There are principally two mechanisms of light modulations that are important in the detection of stress fields, namely polarimetric and interferometric. This is due to the fact that it is the phase and the polarization states of the light transmitted through the fiber that are most sensitive to its variations in refractive index and physical geometry which are modulated by the stress field.

A novel venture in some of these applications is the use of multimode single fiber sensors either imbedded in or firmly attached to the structure being monitored. Here the fiber itself directly

experiences the mechanical perturbations of the structure. Thus, it is certain that there exists a very intimate relation between stresses and strains acting on the fiber and those acting within or on the structures, as the case may be.

From the theory of the mechanics of materials, linear or nearly linear relations should exist for the way the intrinsic material properties and the physical dimensions of the glass fiber are modulated by the mechanical perturbations. Using these relations it should therefore be possible to interpret the variation in the parameters of light output from the fibers using a combination of the electromagnetic theory of propagation in dielectric waveguides and the photoelastic effect, which relates the change in optical properties (refractive index) of a material and an impressed strain. Equations of this nature exist in various publications on specific topics and applications. What has been attempted here is to bring all of these considerations together and to compile those that would specifically serve our purpose of understanding the performance of mechanical perturbation sensors, tailoring those that do not fit our purpose and suggesting some which are not available. This is included in the third chapter of this report. No extensive explanations of the nature and mechanisms of optical transmission through fibers is given. Some of the concepts of stress, strain and the photoelastic effects are however introduced in the second chapter. This forms the first section of this report.

The second section is a report on experiments conducted to establish some basic ideas about the modal domain sensing techniques for strain measurements, being pursued at the Fiber and Elctro-Optics Research Center here at Virginia Tech. These include the work done by Ehrenfeuchter [3] and Shankaranarayanan [4]. In both cases a single multimode fiber was used to monitor stress, specifically vibrations of certain structures [3] and monitoring of acoustic emission in graphite-epoxy coupons [4]. It is evident from these works that the fiber was subjected to a variety of strains. So it was necessary that effects due to specific strains be studied independently so as to be able to model the effects due the combination of strains more thoroughly. So as a prelude to this effort experiments were conducted to subject the fiber to axial strain alone. The

experimental results are presented and the preliminary conclusions are stated. This comprises the fourth and fifth chapters.

1.2 Fundamentals of Optical Transmission in Fibers

Optical fibers are structured as two concentric glass cylinders having slightly different refractive indices. Light waves propagating through a fiber may be visualised as being guided along by sucsessive total internal reflection. The resulting incident and reflected waves then set up interfering standing waves along the transverse direction of the waveguide. The field distribution in the transverse direction remains unchanged as the wave propagates along the axis. This kind of stable standing wave field distribution is called a mode. Such a mode may also be defined as an allowable field configuration for a given waveguide geometry, that satisfies Maxwell's equations and all of the boundary conditions. It is the difference in the two indices and the fiber diameter that determine if a particular mode will be guided or not. The quantities of interest here are the V number of the fiber given by,

$$V = k_0 a \sqrt{n_1^2 - n_2^2},$$

and the propagation constant for a mode N

$$\beta_N = f(V,N),$$

where a is the core diameter and n_1 and n_2 are the core and clad refractive indices, respectively. The V number is a dimensionless quantity which determines how many modes a fiber can support. Note that it is dependent upon the fiber dimension and the refractive index. This is a particularly important parameter in the single fiber multimode sensor applications, to be considered later, as these are precisely the parameters of the fiber that are modulated. β is dependent upon the V

number and is modulated in both polarimetric and interferometric sensors, the two main varieties of sensors. The differences in the propagation constants of the modes cause them to interfere with one another which is an important effect as will become clearer later on.

1.3 Polarimetric Sensing

All such sensors are single mode types supporting the lowest order mode, the HE_{11} mode. From the theory of dielectric waveguides it is known that in actuality a second orthogonal mode is also guided simultaneously. Ideally these orthogonal modes have the same propagation constants due to the isotropic nature of glass. But any anisotropy induced due to an external (or internal) stress field causes these to vary via a change in the circular symmetry of the fiber and a change in refractive index due to the photoelastic effect. This induces a differential phase change between the two guided modes resulting in a birefringence. Monitoring this variation in phase helps us sense the perturbing mechanical field.

1.4 Introduction to 'Modal Domain' Sensing

Modal domain sensing is a method of interferometric sensing. Here the fact that different modes in a fiber have different propagation constants, which are modulated by different amounts by mechanical perturbations, forms the basis of a single multimode fiber acting as an interferometric sensor.

In the conventional Mach-Zender type of interferometer it is the phase difference between the light arriving from two different arms that causes the interference fringe pattern, and the variation in physical length which is mainly responsible for the shift in fringes. By comparison, the far field output pattern of any multimode fiber is observed to be a speckle pattern. It is felt [4] that this speckle pattern is an interference phenomenon between the various modes.

Various experiments involving such multimodal sensors [3,4] have proven that there is a definite rearrangement of this pattern, and a comparison of the experimental observations shows a unique relationship between the mechanical perturbations and the spatial rearrangement of the far field speckle pattern of the output light. This immediately suggests a relationship between the mechanical forces acting on the fiber and the variations in the optical transmission parameters of the fiber undergoing these perturbations. It is therefore necessary that these relations be available to help better quantify the modal domain sensing phenomenon. As a beginning to this end some elementary relations between the mechanical and optical parameters of have been presented.

However a major stumbling block is that the speckle forming mechanism is not too well understood at this moment. Principally due to the complex nature the of mode-mode interaction, it is not possible, in the present work, to also give a proven model for the the speckle rearrangement effect. A practical difficulty is the control of the launching of specific modes in order to know the modes existing in the fiber to be able to model the phenomenon. A more theoretical explanation of this phenomenon may be found in the works of Kapany [5].

But so much is clear that the analysis given in chapter 3 would definitely figure in any further work on this matter, perhaps in some modified form. Therefore, a compilation of this analysis is seen as a helpful supplement in that effort.

2.0 Theoretical Background

2.1 Introduction to Stress and Strain in Solids

The following paragraphs briefly introduce some basic definitions and equations concerning stress and strain in solids. Also stated are optical effects due to these and related equations [7,8].

2.1.1 Stress

A body subjected to external forces has internal forces induced through the material bulk. The average stress σ_m is defined as

$$\sigma_m = F/A, \tag{2.1}$$

where F is the resultant force acting a section of area A. Stress at a point within a body is defined over an area δA as the limit

$$\delta F/\delta A. \tag{2.2}$$

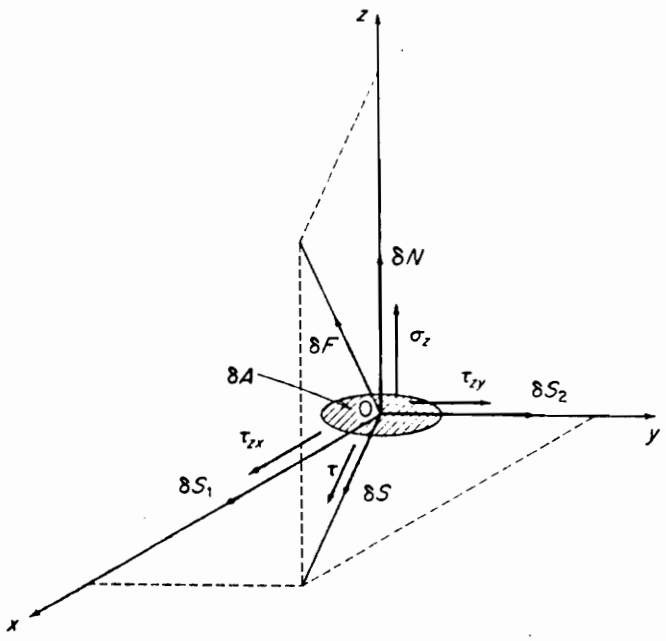

Components of force and stress

Figure 2.

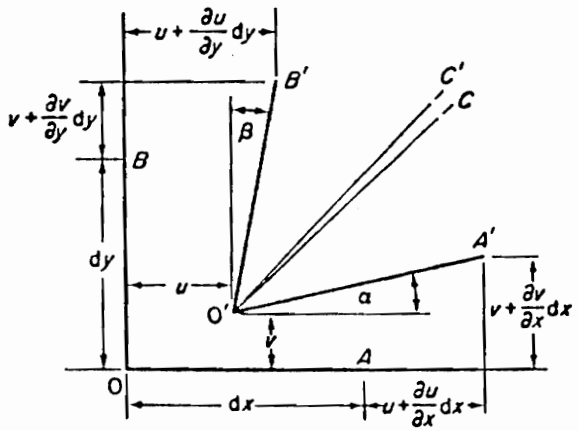

Displacement of line elements in rectangular co-ordinates

Figure 3.

δF may be components δN acting normal to δA and δS acting in the plane of the section. In Figure 2 $\delta N/\delta A$ and $\delta S/\delta A$ are, respectively, the normal and shear stress components. Also δS may be replaced by δS_1 and δS_2 where in the limiting case

$$\delta S_1/\delta A = \tau_{zx}, \tag{2.3}$$

and

$$\delta S_2/\delta A = \tau_{zy} \tag{2.4}$$

The stress components are completely characterized by the forces shown in Figure 2. Here the σ's are the normal stresses and τ's are the shear stresses.

Let us now consider the deformations or strains produced due to the stresses. We start with a spherical element in an unstressed body. If now a uniaxial stress, say tensile, acts on the spere all chords will be changed by amounts proportional to their original lengths. In this way the sphere is transformed into an ellipsoid. The shape of the ellipsoid completely characterizes the state of the stress on the element and can be specified by the independent lengths of the three mutually perpendicular principal axes and their directions.

Displacement of points on the surface of the sphere, in the directions of the axes of the ellipsoid, are purely radial while those of all other points are partly radial and partly tangential. Since radial displacements result from normal stresses and tangential displacements result from shear stresses, it follows that the stresses are purely normal at points in the direction of the principal axes while at all other points both normal and shear stresses are produced. If now the sphere is imagined to be indefinitely reduced and concentrated about a point in a stressed material, there exist three mutually perpendicular directions in which stresses are purely normal. These are referred to as the principal stresses σ_1, σ_2 and σ_3.

2.1.2 Strain

To determine the strains at a point O parallel to one of the co-ordinate plane let us consider, as shown in Figure 3, two infinitesimal line elements OA and OB in a rectangular coordinate system. Let these elements be displaced in the strained body to O′, A′ and B′. If O is displaced by u and v to O′, as shown, we write the corrosponding displacements of A′ and B′ as

$$u + \frac{\delta u}{\delta} x dx; v + \frac{\delta v}{\delta} x dx. \qquad 2.5$$

One way of understanding the above expressions is recognizing them as the first two terms of a Taylor series expansion. We define the linear or normal strain as the change in length per unit length. Now the change in the length of element OA in the x direction is given by (δu/δx)dx. Strain therefore is given by (δu/δx)dx/dx, or normal strain in the x direction is given as

$$\varepsilon_x = \frac{\delta u}{\delta x}. \qquad 2.6$$

The shear strain is defined as the sum of the angles $\alpha + \beta$. By considering the two right-angled triangles which include the angles α and β, assuming these angles to be small, we write the shear stresses as

$$\gamma_{xy} = \alpha + \beta = (\frac{\delta v}{\delta x}) + (\frac{\delta u}{\delta y}). \qquad 2.7$$

In this way we can relate all six components of strain at a point as

$$\varepsilon_x = \frac{\delta u}{\delta x} \quad \varepsilon_y = \frac{\delta v}{\delta y} \quad \varepsilon_z = \delta\frac{w}{\delta z}, \qquad 2.8$$

$$\gamma_{xy} = \delta u/\delta x + \delta v/\delta y \quad \gamma_{yz} = (\delta w/\delta y) + (\delta v/\delta z) \quad \gamma_{zx} = (\delta u/\delta z) + (\delta v/\delta x), \qquad 2.9$$

where u, v, and w are the components of displacements of the point parallel to the x, y and z axes.

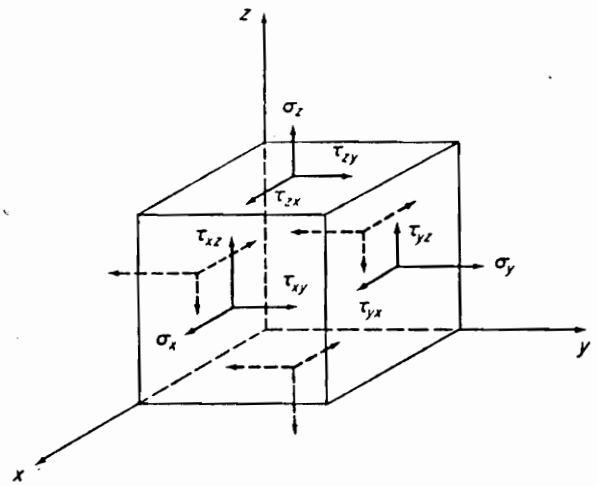

Stress components in rectangular co-ordinates on an infinitesimal element

Figure 4.

2.1.3 Relation Between Stress and Strain

All bodies are deformed when loaded. An elastic material is one in which all deformations vanish when load is removed. In the theory of elasticity it is usual to postulate also that in an elastic material the strains are proportional to the applied load and the elastic properties are the same in all directions. Such a material is said to be isotropic. These properties hold over a certain stress range known as the elastic limit.

Consider a long prismatic bar under uniaxial stress δ_x along the x axis. Within the elastic range the longitudinal strain is

$$\varepsilon_x = \sigma_x/E, \tag{2.10}$$

which is the well known Hooke's law relating stress and strain. Here E is a constant called the modulus of elasticity. The lateral strains $\varepsilon_y + \varepsilon_z$ due to σ_x are given by

$$\varepsilon_y = \varepsilon_z = -\nu\varepsilon_x, \tag{2.11}$$

where ν is Poisson's ratio. The generalized expression for the three dimensional case is given by

$$\varepsilon_x = [\sigma_x - \nu(\sigma_y + \sigma_z)], \tag{2.12}$$

and similarly for the other two directions. Applying these results to shear strains produced by shear stresses we have

$$\gamma_{xy} = \tau_{xy}/G\gamma_{yz} = \tau_{yz}/G\gamma_{zx} = \tau_{zx}/G, \tag{2.13}$$

where G is called the shear modulus or modulus of rigidity.

As a final equation given below are the relations between the polar stresses and their associated strains.

$$\sigma_r^i = \varepsilon_r^i(\lambda^i + 2\mu^i) + \varepsilon_z^i\lambda^i, \qquad \textit{and}$$
$$\sigma_\theta^i = \varepsilon_r^i\lambda^i + \varepsilon_\theta^i(\lambda^i + 2\mu^i) + \varepsilon_z^i\lambda^i, \sigma_z^i = \varepsilon_r^i\lambda^i + \varepsilon_\theta^i\lambda^i + \varepsilon_z^i(\lambda^i + 2\mu^i) \tag{2.14}$$

where i = 1,2 refers to the core and clad region of an optical fiber, respectively, and

$$\lambda^i = \frac{\nu^i E^i}{(1 + \nu^i)(1 - 2\nu^i)}, \qquad \mu^i = \frac{E^i}{2}(1 + \nu^i). \tag{2.15}$$

Thus it is easily seen from the above equations that the stress-strain relations are essentially linear (in the elastic range).

2.2 *Optics of Photoelasticity*

Many non-crystalline transparent materials which are ordinarily optically isotropic become anisotropic temporarily when subjected to a stress. This usually vanishes as soon as the stress is removed. The mechanically-induced stress or strain cause intermolecular variations in the structure of the body which alters its optical isotropic character. There exist linear relations between the variations of the refractive index, which is treated here as tensor, and the stresses. These relations are

$$\begin{aligned} n_1 - n &= C_1\sigma_1 + C_2(\sigma_2 + \sigma_3), \\ n_2 - n &= C_1\sigma_2 + C_2(\sigma_1 + \sigma_3), \\ n_3 - n &= C_1\sigma_3 + C_2(\sigma_1 + \sigma_2). \end{aligned} \tag{2.16}$$

This is known as the stress optical law. Here C_1 and C_2 are called the stress-optic coefficients and have the inverse units of stress.

Another associated effect is the strain optic effect which gives the relation between change in refractive index and the strain and is given as [9],

$$\Delta\left(\frac{1}{n^2}\right)_i = \sum_{j=1}^{6} p_{ij}\varepsilon_j. \qquad 2.17$$

Here P_{ij} is the strain optic coefficient. With no shear strain $\varepsilon_4 = \varepsilon_5 = \varepsilon_6 = 0$. We need consider only the i,j = 1,2,3 elements and for an isotropic homogeneous material it is given as

$$P_{ij} = \begin{bmatrix} p_{11} & p_{12} & p_{12} \\ p_{12} & p_{11} & p_{12} \\ p_{12} & p_{12} & p_{11} \end{bmatrix}$$

W have therefore seen in this chapter the relations between the stress and strain and also introduced the basic equations relating variation of refractive index of isotropic materials with stress and also the associated strains.

3.0 Mechanisms of Modulation

Described below are the two main mechanisms of light modulation that occur in optical fibers under the influence of mechanical perturbations. Relations are given between the stress or strain and the resulting variations in the optical transmission parameters of the fibers.

3.1 Phase modulation mechanisms in fibers

Phase modulation is intrinsically one of the most sensitive measures of environmental changes using optical fibers. There are basically two configurations of fiber sensors that may be used to monitor the phase effects. The first is as the two arms of a Mach-Zehnder interferometer using single mode fibers. The second is the single fiber configuration using multimode fibers which exploits the variation of phase between the different modes in the fiber.

Phase modulation effects are basically due to variations in

physical length of the fiber due to axial strain,

radial dimensions of the fiber due to radial strain, and

refractive index via the photoelsatic effect.

Let us first consider the phase modulation effects in the Mach-Zehnder configuration. Here the basic equation for the phase φ of the output of the fiber is given by [9].

$$\varphi = \beta \times L, \tag{3.1}$$

where β is the single mode propagation constant of light in the fiber and L the length of the fiber. Also let n be the refractive index of the core, k_0 the free space propagation constant and a the core diameter.

Let the fiber be under isotropic stress due to some external condition with no shear components. The change in phase due to strain may be written as [9]

$$\Delta\varphi = \beta\Delta L + L\Delta\beta. \tag{3.2}$$

Here the first term accounts for the physical change in length due to the strain. Here ΔL may be simply written as

$$\Delta L = \varepsilon_z L. \tag{3.3}$$

The second term involves change in phase due to change in β which occurs mainly due to two effects

the variation in refractive index via photoelastic effects

the change in radial dimensions.

It may be represented by

$$L\Delta\beta = L\frac{d\beta}{dn}\Delta n + L\frac{d\beta}{dD}\Delta a. \qquad 3.4$$

The first term in the above expression is due to the variation in the refractive index in the z direction, due to the photoelastic effects. This is given as [9]

$$\Delta n = \frac{1}{2}n^2[\varepsilon_z p_{12} + \varepsilon_x(p_{12} + p_{11})]. \qquad 3.5$$

Here it should be remembered that $\varepsilon_x = \varepsilon_y$.

Now β is given by $\beta = k_0 n_{eff}$ where n_{eff} lies between the core and cladding indices. But as these differ only by 1% or so we can write it as $\beta = k_0 n$ and therefore

$$d\beta/dn = k_0.$$

The second term gives the change in β due to change in diameter of the core. Here the change in diameter Δa is simply

$$\Delta a = \varepsilon_x a.$$

$d\beta/da$ is evaluated as

$$\frac{d\beta}{da} = (V^3/2\beta a^3)\frac{db}{dV}, \qquad 3.6$$

where V is v-number given as $V = k_0 a(n_1 - n_2)^{1/2}$, $b = \dfrac{\beta^2/k_0^2 - n_2^2}{n_2^2} - n_1^2$ and db/dV is the slope of the b - V curve[9].

Therefore $L\Delta\beta$ may be written as

$$L\Delta\beta = Lk_0\frac{1}{2}n^2\varepsilon_z P_{12} + \varepsilon_x(P_{12} + P_{11}) + L\varepsilon_x V^3/2\beta a^2\frac{db}{dV} \qquad 3.7$$

Therefore change in phase per unit length of fiber due to the various strain components may be written as

$$\Delta\frac{\varphi}{L} = \varepsilon_z(\beta + \frac{1}{2}n^2k_0P_{12}) + \varepsilon_x k_0 n^2(P_{12} + P_{11})\frac{V^3}{2\beta a^2}\frac{db}{dV}. \qquad 3.8$$

We now take up the case of the multimode single fiber configuration. For this the key relation is the one given in Eqn. 3.4. But here as both the 'arms' of the interferometer are the same fiber, change in length effects all the modes in the same manner. So we will consider the effect due to change in β only. This is because each mode has a different propagation constant and the n_{eff} is given as [10].

$$n_{eff}^N = n_1\{1 - \Delta(\frac{N+1}{N_m+1})^2\},$$

where

$$\Delta = \frac{n_1^2 - n_2^2}{2n_1^2} \cong \frac{n_1 - n_2}{n_1},$$

$$N_m = \frac{V}{\pi/2}$$

where V is the v-number of the fiber.

It has been shown [11] that in such mode-mode interactions effect of change in fiber diameter on change in β for a mode may be neglected for the case of a circularly symmetric plane strain. Using this result we may derive for change in phase for given mode, an expression, as follows.

$$\frac{\Delta\varphi}{L} = \Delta\beta$$

Note that as this expression contains variations due only one term alone compared to the three terms in Eqn. 3.4 it could well be expected that the sensitivity of the single fiber 'interferometer' to be less than the conventiontional Mach-Zehnder type which is indeed verified in practice. In the development of Eqn 3.8 we assumed that n_{eff} was the same as n the core index. But in this case it is the difference in the variation in the of refractive indices that causes phase difference between modes. So to account for this we derive the relation d β/dn using the expression for n_{eff} So

$$\begin{aligned}\beta &= k_0 n_{eff} \\ &= k_0 \left\{ n_1 - \frac{(N-1)\lambda^2 (n_1 - n_2)}{(4a\sqrt{n_1^2 - n_2^2} + \lambda)^2} \right\},\end{aligned} \tag{3.9}$$

where N is the mode number. So as β is a function of the core diameter a, the core and cladding indexes n_1 and n_2, we may derive the total derivative of β

$$\Delta\beta = \frac{\delta\beta}{\delta n_1} dn_1 + \frac{\delta\beta}{\delta n_2} dn_2 + \frac{\delta\beta}{\delta a} da. \tag{3.10}$$

We use the expressions derived by [12] for the dn's, which is $n_z^i = n^i + C_2^i(\sigma_{rr}^i + \sigma_{\theta\theta}^i)$ where i = 1,2 refer to the core and clad regions respectively , C_2 the transverse photoelastic constant and n_z the index of refraction along the z axis in the stressed state. Also we write da as σ_{zz}/E where E is the Youngs modulus. By partial differentiaion of Eqn. 3.9 we obtain the following expression for change β for a mode N

$$\Delta\beta_N = \frac{k_0}{f\sqrt{n_1^2 - n_2^2}} \{ f\sqrt{n_1^2 - n_2^2} - \{ q[4a(n_1^2 - n_2^2) + \lambda\sqrt{n_1^2 - n_2^2}] \times$$

$$[C_2^{(1)}(\sigma_{rr}^{(1)} + \sigma_{\theta\theta}^{(1)}) - C_2^{(1)}(\sigma_{rr}^{(2)} + \sigma_{\theta\theta}^{(2)})]\} -$$

$$\{8aq(n_1 - n_2)[n_1 C_2^{(1)}(\sigma_{rr}^{(1)} + \sigma_{\theta\theta}^{(1)}) - n_2 C_2^{(2)}(\sigma_{rr}^{(2)} + \sigma_{\theta\theta}^{(2)})]\} +$$

$$[4aq(n_1 - n_2)(n_1^2 - n_2^2)\frac{\sigma_{zz}}{E}]\}, \tag{3.11}$$

where $f = (4a\sqrt{n_1^2 - n_2^2} + \lambda)^3$ and $q = (N - 1)\lambda^2$.

Here the expression is in the cylindrical coordinates and unlike the others it has terms for stress an the corrospondding stress-optic coefficients. These may be converted to strain terms using Hookes law and the relation between stress and strain optic coefficients $P_{11} = -2EC_1/n^3$ and $P_{12} = -2EC_2/n^3$ It should however be mentioned that this expression holds only if all the quantities involved are known precisely and the assumed conditions of uniform radial pressure is satisfied.

3.2 *Mechanisms of Polarization Modulation*

Polarimetric fiber-optic sensors detect the presence of a physical field via a change in state of polarization of light propagating through a single mode fiber. It must be noted that even in a single mode fiber two 'modes' perpendicularly polarized to each other may propagate. It is the differential change between these that form the mechanism of sensing. The physical field to be sensed causes an asymmetric stress in the fiber cross section thus unequally changing the phase velocities of the orthogonal palarization modes. The mechanism may therefore be analysed similar to the phase modulation.

The following discussion follows that of [13] for a step index fiber under radial pressure which is acting alona diameter.

For this purpose we limit our examination around the center of the fiber as most of the energy in a step index fiber is almost entirely confined to the core. We may therefore write the change in refractive indices as that involving only n_1 as

$$n_x = n_1 + (C_1\sigma_x + C_2\sigma_y)$$

$$n_x = n_1 + (C_1\sigma y + C_2\sigma_x).$$

Now writing the β's as

$$\beta^x = n_x k_0, \ \beta^y = n_y k_0,$$

we can write the birefringence as

$$\begin{aligned} \Delta\beta &= \beta^y - \beta^x \\ &= \sigma_y(C_1 - C_2) + \sigma_x(C_2 - C_1) \end{aligned} \qquad 3.12$$

The components of principal stress around the center may be approximated as

$$\sigma_x = \frac{-3f_0}{\pi b}, \quad \sigma_y = \frac{f_0}{\pi b},$$

where f_0 is the external force per unit length. Therefore Eqn 3.12 may be written as

$$\Delta\beta = \frac{8}{\lambda b}(C_1 - C_2)f_0. \qquad 3.13$$

This is also equal to

$$\Delta\beta = \frac{4n_1^2}{\pi}\frac{1+\nu}{E}(P_{12} - P_{11})\frac{f}{2b}, \qquad 3.14$$

where ν is the Poisson's ratio.

The induced linear birefringence may also given by.

$$\Delta\beta = \Delta\beta^y - \Delta\beta^x = -k_0 n_0^3 l\frac{(P_{11} - P_{22})}{2}(\varepsilon_1 - \varepsilon_2) \qquad 3.15$$

where ε's are the principal strains given as

$$\varepsilon_{1(2)} = \left\{ \frac{\varepsilon_{rr} + \varepsilon_{\theta\theta}}{2} + (-)\frac{1}{2}[(\varepsilon_{rr} - \varepsilon_{\theta\theta})^2 + 4\varepsilon_{r\theta}^2] \right\}, \tag{3.16}$$

where $\varepsilon_{rr}, \varepsilon_{\theta\theta}, \varepsilon_{r\theta}$ are the strains in cylindrical coordinates. The P's are the strain optic coefficients. Eqn. 3.14 may easily be got from Eqn. 3.12 by replacing the stress by the strain terms. Eqn 3.14 then becomes

$$\Delta\beta = -k_0 n_0^3 l \frac{(P_{11} - P_{12})}{2}(\varepsilon_{rr} - \varepsilon_{\theta\theta})^2. \tag{3.17}$$

The change in two orthogonal modes is given as

$$\begin{aligned} \Delta\beta^x &= k_0 n_0^3 l(P_{12}\varepsilon_1 + P_{11}\varepsilon_2)/2 \\ \Delta\beta^y &= -k_0 n_0^3 l(P_{11}\varepsilon_1 + P_{12}\varepsilon_2)/2. \end{aligned} \tag{3.18}$$

Twisting a fiber around its axis with a uniform rate $2\pi N$ rad/m where N is the number of turns per meter will induce will induce a circular birefringence unlike in the other cases where the birefringence was linear. The induced birefringence is given by [13].

$$\Delta\beta = \frac{n_1^2}{2}(P_{11} - P_{12})2\pi N \tag{3.19}$$

We have also for a bend induced birefringence a normalized value.

$$\frac{\Delta\beta}{\beta} = \frac{n_1^2}{4}(P_{11} - P_{12})(1 + \nu)(a/R)^2, \tag{3.20}$$

where R is the bend radius and β the mean of β_y, β_x For bending under tension, an additional normalized birefringence is given as

$$\frac{\delta\beta}{\beta} = \frac{n_1^2}{2}(P_{11} - P_{12})\frac{(1 + \nu)(2 - 3\nu)}{1 - \nu}(b/R_0)\varepsilon_{zz}. \tag{3.21}$$

Thus we have achieved upto a fair degree of completeness the derivation of equations relating the various optical transmission parameters like refractive index, phase, propagation constant and birefringence to the mechanical perturbation parameters stress or strain. Given below is a compilation of the all the important relations that have been derived earlier.

Refractive Index

$$n_r = n_0 + (C_1\sigma_{rr} + C_2\sigma_{\theta\theta})$$
$$n_\theta = n_0 + (C_1\sigma_{\theta\theta} + C_2\sigma_{rr})$$
$$n_z = n_0 + C_2(\sigma_{rr} + \sigma_{\theta\theta})$$

Phase

$$\frac{\Delta\varphi}{L} = \varepsilon_{zz}(\beta + \frac{1}{2}n^2k_0P_{12}) + \varepsilon_x k_0 n^2(P_{12} + P_{11})\frac{V^3}{2}\beta a^2\frac{db}{dV}$$

Propagation constant

$$\Delta\beta_N = \frac{k_0}{f\sqrt{n_1^2 - n_2^2}}\{f\sqrt{n_1^2 - n_2^2} - \{q[4a(n_1^2 - n_2^2) + \lambda\sqrt{n_1^2 - n_2^2}] \times$$

$$[C_2^{(1)}(\sigma_{rr}^{(1)} + \sigma_{\theta\theta}^{(1)}) - C_2^{(1)}(\sigma_{rr}^{(2)} + \sigma_{\theta\theta}^{(2)})]\} -$$

$$\{8aq(n_1 - n_2)[n_1C_2^{(1)}(\sigma_{rr}^{(1)} + \sigma_{\theta\theta}^{(1)}) - n_2C_2^{(2)}(\sigma_{rr}^{(2)} + \sigma_{\theta\theta}^{(2)})]\} +$$

$$[4aq(n_1 - n_2)(n_1^2 - n_2{}^2)\frac{\sigma_{zz}}{E}]\}$$

Birefringence

$$\Delta\beta = \frac{8}{\lambda b}(C_1 - C_2)f_0$$

this is also equal to

$$\Delta\beta = \frac{4n_1^2}{\pi}\frac{1+\nu}{E}(P_{12} - P_{11})\frac{f}{2b}$$

where ν is the Poisson's ratio of Silica. It may also be given as

$$\Delta\beta = -k_0 n_0^3 l \frac{(P_{11} - P_{12})}{2}(\varepsilon_{rr} - \varepsilon_{\theta\theta})^2$$

Twist induced birefringence is given by

$$\Delta\beta = \frac{n_1^2}{2}(P_{11} - P_{12})2\pi N$$

We have also for a bend induced birefringence a normalized value.

$$\frac{\Delta\beta}{\beta} = \frac{n_1^2}{4}(P_{11} - P_{12})(1+\nu)(a/R)^2$$

where R is the bend radius and β the mean of β_y and β_x For a bending under tension an additional normalized birefringence is given as

$$\frac{\delta\beta}{\beta} = \frac{n_1^2}{2}(P_{11} - P_{12})\frac{(1+\nu)(2-3\nu)}{1-\nu}(b/R_0)\varepsilon_{zz}$$

It may be mentioned here that following the development of these relations it is realized that these equations may appear in any theory relating to the 'modal domain' sensing techniques perhaps in some modified form without, however, any drastic changes.

4.0 Experiment and Observations

4.1 Motivation and Reasons

Modal domain methods involving mode-mode interference effects are being actively investigated at the Fiber and Electro-Optics Research Center at Virginia Tech for applications in the sensing of vibration in structures and acoustic emission in composites [3,4]. In the above applications fibers are firmly bonded to the specimen and experience a combination of strains when the specimens are subjected to perturbations.

A question that arises in these applications is if the observed signals are a function of the well documented bend loss effects. To ascertain this it was necessary to conduct experiments which would not involve any bend loss effects, or at least be limited to only some non-varying kinds. Research on these applications also suggested that the axial strain to be a major factor contributing to observed effects. For example, it has also been noted that ability of the fiber to exhibit the 'modal' sensing effects due to both vibrations of structures and due to acoustic emission was more pronounced when the sensing fiber was bonded in a state of slight tension. For both these reasons

it was felt that it may be pertinent to monitor the 'modal' effects created by subjecting a bare fiber to quasi-static tensile loads.

4.2 Apparatus

A few-mode optical fiber (core diameter 8 microns; clad diameter 125 microns; NA$\cong$0.10, V$\cong$4) was chosen as the most suitable candidate for this purpose as it was the same kind of fiber used in [3,4] and also the output pattern was such that it was well defined and could be easily reproduced. The pattern was a four lobed configuration as shown in Figure 5.

The tensile loading was provided by a conventional tensile testing machine - the J.J.Lloyd T20000 model. The machine applies a tensile load to a specimen held between two grips. The applied tension and extension from a set position is displayed by a microprocessor unit. The rate at which the tension is applied may be adjusted as required between 0.1 and 50 mm/m in steps of 0.1 mm. The grips may also be driven back to release the applied tension also adjustable between the same range. For our purpose special grips were used to enable the fiber to be axially strained without slipping and without excessive concentration of stress at the grips.

A 5.0 cm section of the fiber was mounted on the tensile testing machine, as shown in Figure 5. Another section of the fiber was bonded to the surface of a steel cantilever beam (t = 0.65 mm, L = 16.0 cm). This was similar to the one used by [3]. The fiber was fixed as a loop as shown in the figure to eliminate a dangling end and increase the length of interaction. This provided a mechanism to subject the fiber to low frequency strain variations of the order of 10^{-4}. That is to say that the fiber could be subjected to an oscillatory tension around the relatively larger magnitudes of tension provided by the machine.

The tensile testing machine range of 0-50 mm/min displacement (in steps of 0.1 mm/min) corresponds to a lower limit of 10^{-5}/sec strain for a 20 cm interaction length. A Nicolet digital storage oscilloscope was used to monitor and store the detector output.

4.3 Experiment and Observations

The tensile testing machine was operated at speeds of 0.5, 1.0 and 2.0 mm/min to simulate quasi-static loading conditions. A redistribution of the mode pattern was observed. The lobes rotated with speeds proportional to the pulling speeds.

The intensity of the spatially filtered pattern (i.e. the intensity of a small fixed segment of the pattern) was observed to vary in a sinusoidal manner. Because of the known strain rate, the intensity signal could be related directly to the axial strain in the fiber. Output signals for displacement rates of 0.5 and 1.0 mm/min are shown in Figures 6 and 7 respectively. Note that the average time period of the signals is inversely proportional to the displacement rates. This confirms that the change in the intensity mode pattern is due to strain. Note that the time period for the faster strain rate of 1.0 mm/min is almost exactly half the period for the slower case.

To study reversability and repeatability, the strain was applied and removed twice at the same rates. The output signals during tension and release are shown in Figures 8 and 9. Note the excellent reciprocity indicated by the inverted waveforms. The excellent tracking of the strain in both 'directions' reveals the linear relation between the change in the mode pattern and small axial strains.

Note that the intensity is periodic for strains of the order of 10^{-3} and the rate of change of intensity with strain is lowest at the 'peaks' and highest in the middle. A low-frequency varying strain of the

order of 10^{-4} was generated in the fiber by vibrating the cantilever beam. This was done for two different strain conditions, one slightly above 'peak' and the other in the 'middle' of the sinusoidal variation of the output of the detector monitoring the far field speckle pattern rotation. The output signals are shown in Fig. 10. Note the higher amplitude for the middle case where the rate of change of intensity with strain was highest. The phenomenon reported by [3] was also confirmed as the variation of the signal was at vibrating frequency of the beam.

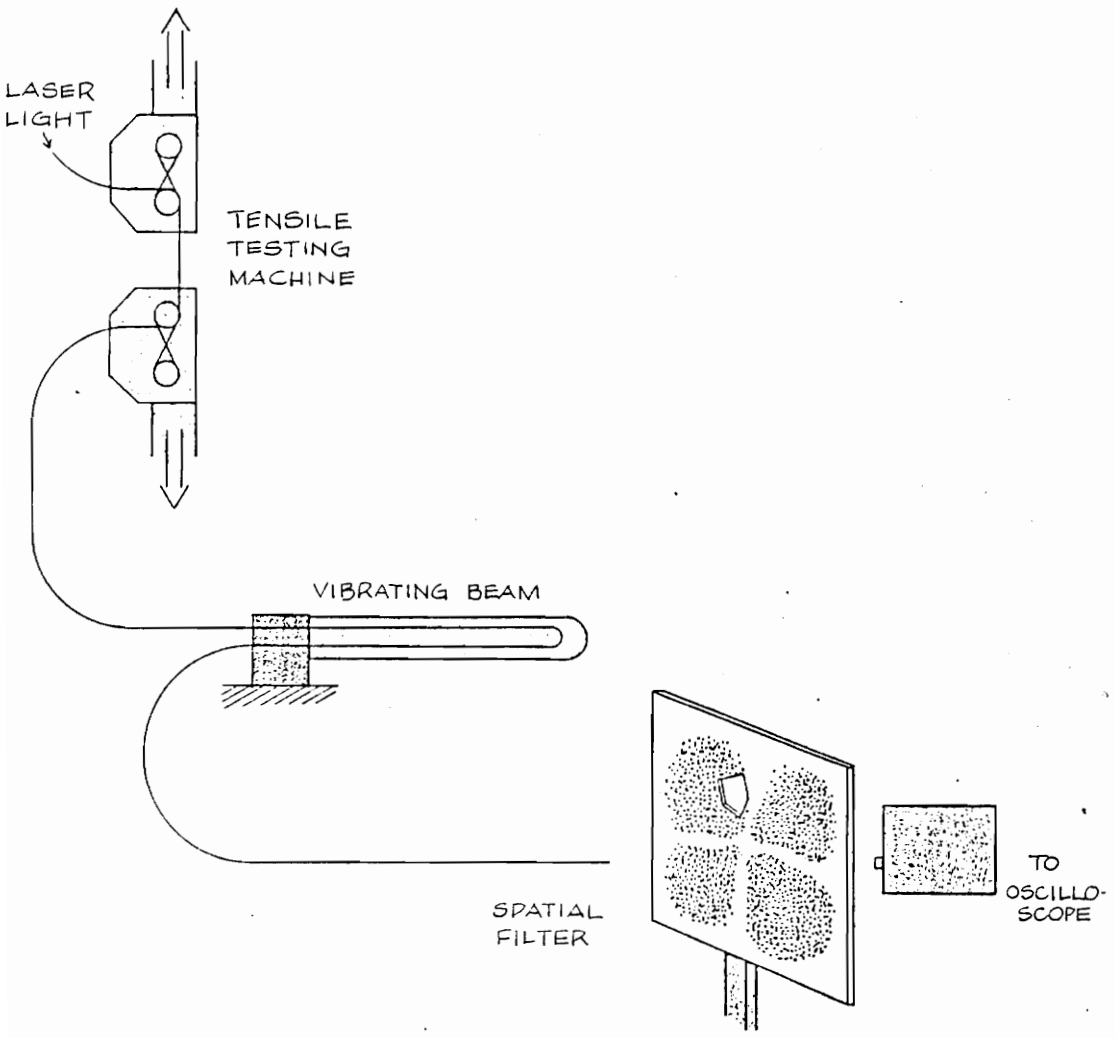

Figure 5. Experimental set-up.

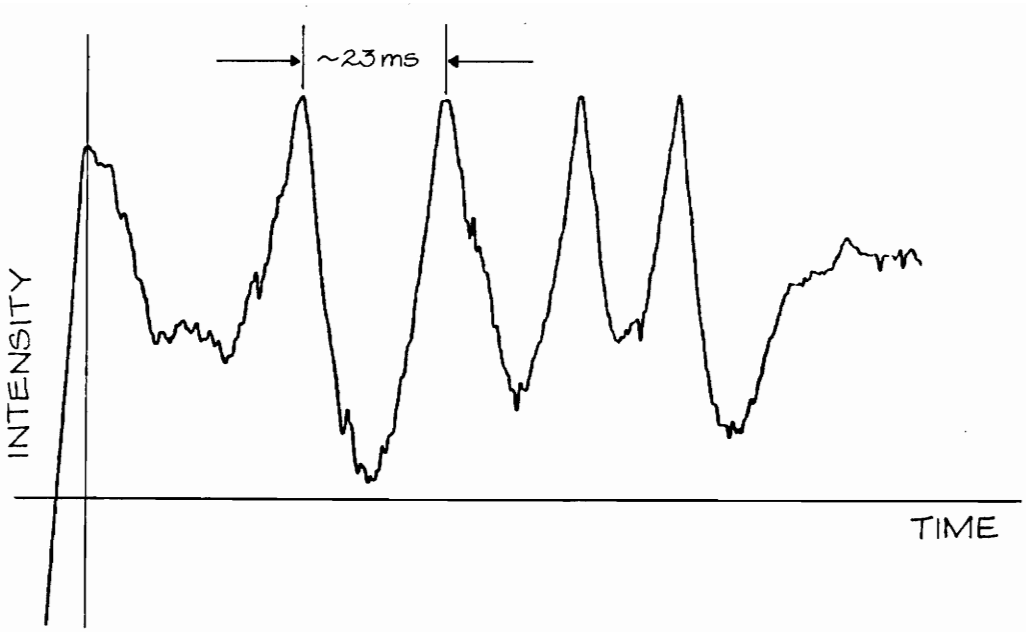

Figure 6. Output for 0.5 mm/min displacement rate.

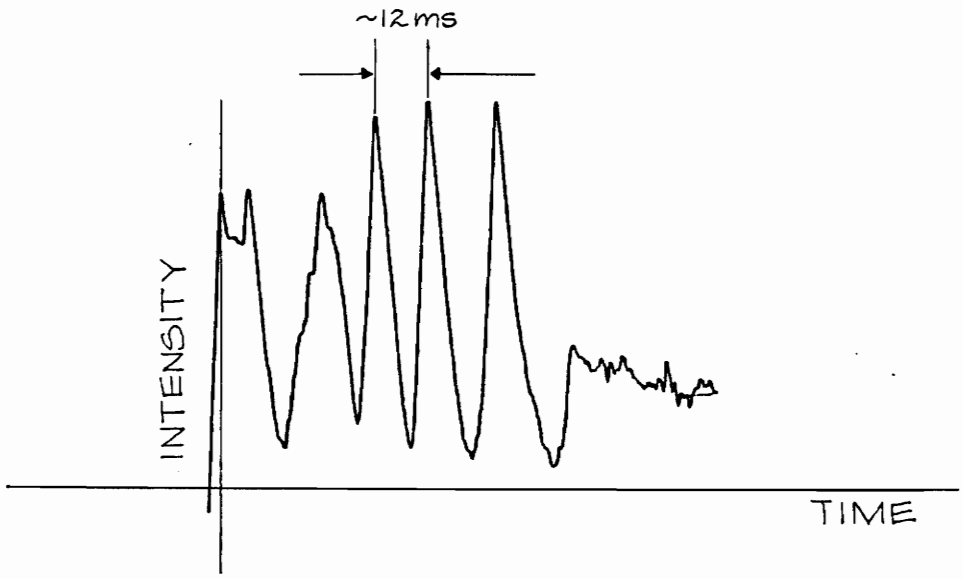

Figure 7. Output for 1.0 mm/min displacement rate.

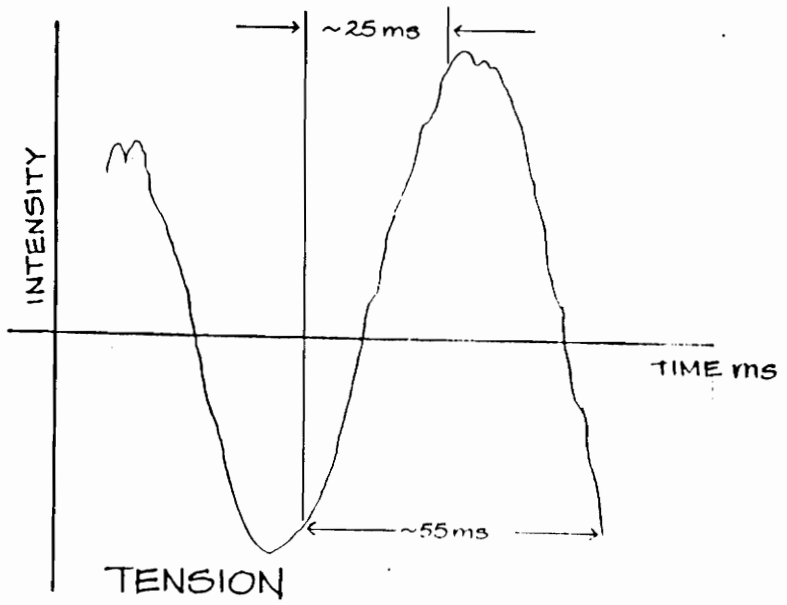

Figure 8. Output as tension is applied.

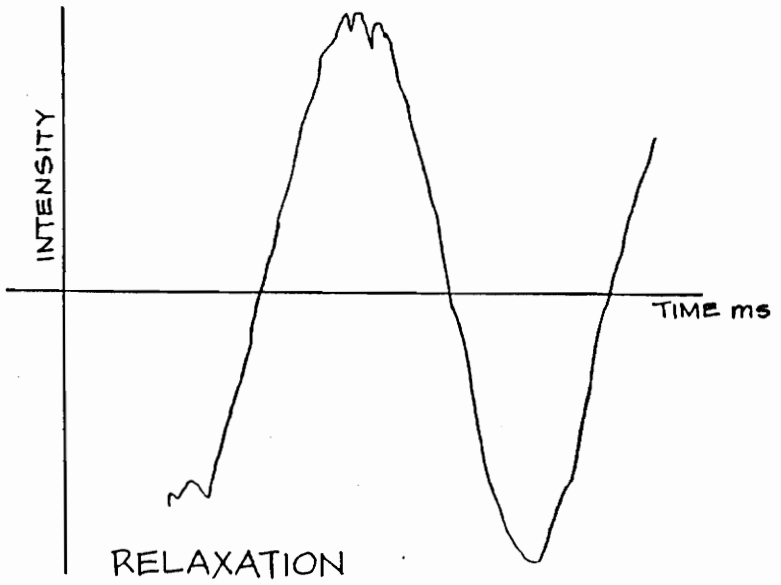

Figure 9. Output as tension is released.

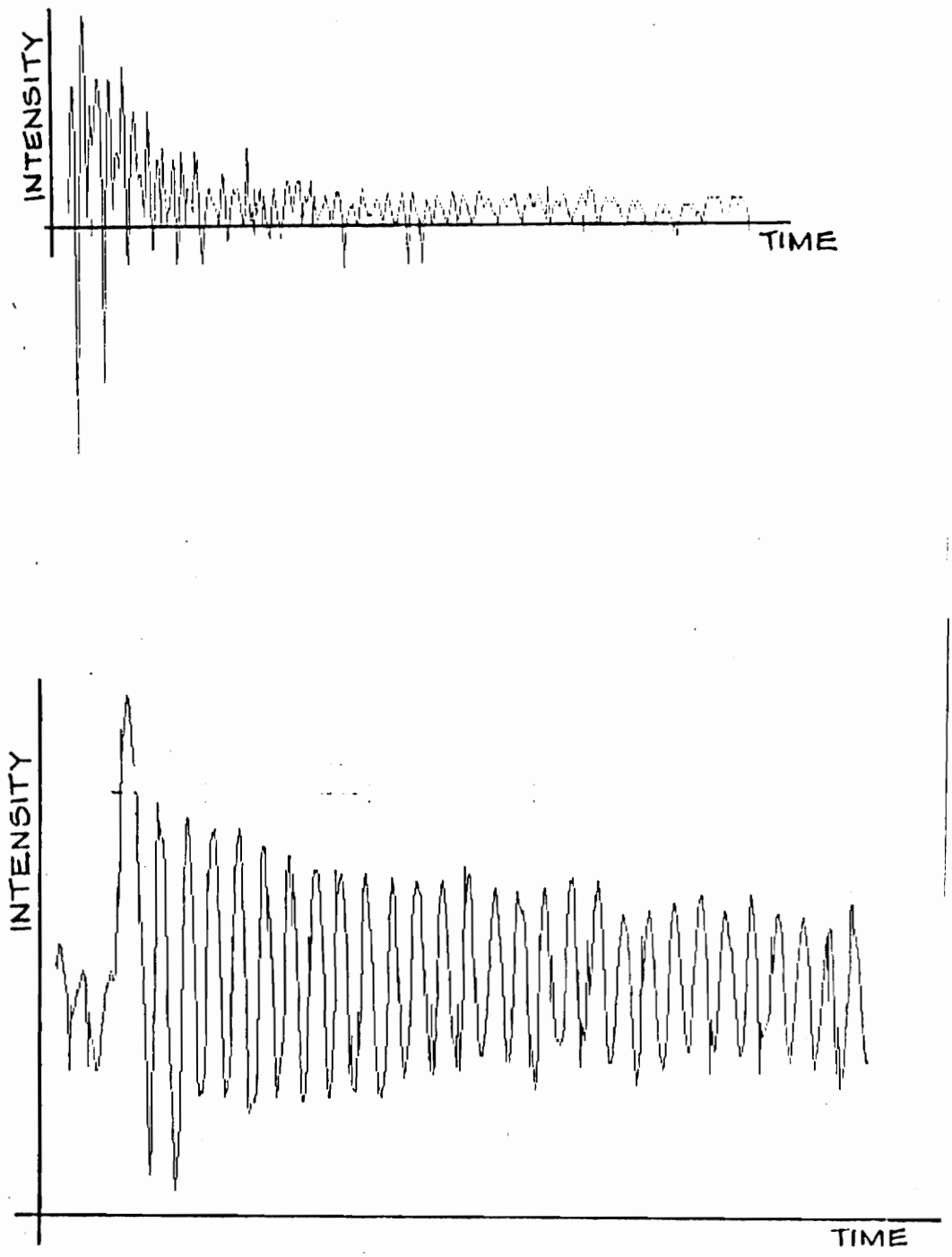

Figure 10. Output due to vibrating beam at the two states of tension.

5.0 Conclusions

A modal modulation effect due to axial strain in an optical fiber been observed. The relation between the effect of prestressing the fiber axially and the sensitivity of this 'modal' mechanism to monitor flexural deflections is reported. We are now in a position to offer some preliminary models for the further exploitation of this sensing technique.

5.1 Discussion

For $V \cong 4$, we have seven modes HE_{11}, TE_{01}, TM_{01}, HE_{21}, HE_{12}, EH_{11}, and HE_{31} [10]. The mode pattern used by us with four nodal lines is probably due to the mode combination of HE_{31} and EH_{11} and this mode combination rotates along the fiber [5]. Due to the phase modulation [5] and polarization modulation resulting from strain, there is a change in the mode pattern. A rotation in the mode pattern is observed at the detector if a spatial filter is located on the nodal line. [5] (A nodal line may simply be understood as the dark regions between the 'lobes' of the output pattern.) We could relate the sinusoidal variation of the intensity to the rotation of the nodal line past the spatial filter. A combination of modes should result in a symmetric pattern and the varying

intensities of the quadrants results from non-circularities of the fiber. It is interesting that the rotation of the nodal line corresponds well to the strain rate as was observed.

The rotation of the mode pattern is also reversible and rotates in the opposite direction when the strain is released. The tensile testing machine does take a finite time to reverse the strain and though we could observe the effect of strain on the fiber, our timing capabilities do not allow a measurement of any hysteresis effects in the reversal.

For small a.c. excitations at an existent 'd.c.' strain, we have observed similarities to typical biasing and load-line situations in a transistor. That is, there seems to be a certain prestressed condition of the the optical fiber which makes it more sensitive to such modal methods of sensing. More importantly the required stress condition seems to be indicated by the rotation of the mode pattern. Just as setting the Q point is important in the operation of a transistor it seems necessary to bias the fiber by prestressing it to be able to monitor such vibrational phenomenon as indicated above. The response to small strains can be tailored by controlling a quasi-static strain elsewhere on the fiber. This could very well be a piezoelectric cylinder in sensor applications.

This principle could be used in a sensor with one region of the fiber exposed to axial strain and another exposed to a controlled strain (e.g. bonded to PVDF cable or wound on a PZT cylinder). If the controlled strain is increased to some value, then by release or enhancement of strain we could nullify the strain changes in the sensing region. This gives us a convenient electrical signal from the control loop as the sensor output. We have an advantage of not having to deal with varying intensities between nodal lines.

5.2 *Conclusion*

- We have observed a sinusoidal variation of the detector output from a modal domain detection set-up for small, slowly increasing axial strain. This signal shows reciprocity when the strain is applied and removed.
- This observation indicates that the strain produces a simple rotation in the far field output pattern of te fiber.
- We have subjected the fiber to small a.c. strains under different d.c. strains and have noted the conditions of bias required for such applications.
- We have been able to identify , on the modal pattern, a region of most sensitivity for sensing of flexural vibrations.
- We have indicated a simple model to explain the mode pattern and axial strain effects.

5.3 *Suggestions*

As has been mentioned earlier the observed effect of pattern 'rotation' could be combination of phase and polarization effects [5]. To confirm this, further experiments of a similar nature would be useful. The same experiment could be performed, but this time seperating the far field output of the fiber into the two orthogonal eigen modes by passing it through a polarizing element such as a polarizing beamsplitter. A comparative study of the behaviour of these orthogonal componants should indicate the contribution of each of these eigenmodes to the total effect of rotation that has been observed. Indeed even more signifcant it would check out the validity of this effect being dependent on polarization at all.

Another variation to the set up used in this study would be to use coupler at the output so as to seperate out the higher order modes and the lower order ones and the observe varations, if any, in the two outputs. This should give us an indication of the contributions of the lower and higher order modes to the effects described in this report. In fact using the information from the mode patterns in [5] we may also be able to understand how the modes get transferred at the coupler as axial tension is being applied to it.

Indeed it would be worthwhile performing all the experiments of [3,4] to be able to quantify the required pre-stress conditions on the sensing fiber to tailor the sensitivity of this method for these specific applications. A result of significance would be to be able to quantify specific pattern variations and relate them to existing conditions of tension in the optical fiber. A specific experiment suggested is to vibrate the portion of the fiber under tension at a known frequency by using, for example, a tuning fork. This should also simulate the acoustic emission phenomenon of [4].

A related experiment would be to verify if similar phenomenon are observed if the same or similar fiber is attached to a magnetostrictive material and exposed to a magnetic field. As the material expands the optical fiber should also experience the same strain.

6.0 References

[1] T. G. Giallorenzi, et al., "Optical Fiber Sensor Technology", IEEE Transactions on Microwave Theory and Techniques, Vol MTT-30, NO. 4 April 1982.

[2] B.Culshaw, "Optical Fiber Sensing and Signal Processing", pp 73-86, Peter Perigrinus, 1982.

[3] Paul Ehrenfeuchter, Masters Thesis, Virginia Tech , December 1986.

[4] N. K. Shankarnarayanan et al., "Optical Fiber Modal Domain Detection of Stress Waves", Proceedings, IEEE Ultrasonics Symposium (Williamsburg, VA), November 1986.

[5] N.S.Kapany and J.J.Burke, "Optical Waveguides", Academic Press 1972.

[6] N.K. Shankarnarayanan, Internal Report, Fiber & Electro-Optics Research Center, Virginia Tech.

[7] A.Kuske and G.Robertson, "Photoelastic Stress Analysis",
John Wiley & Sons, 1974.

[8] Theocaris and Gdoutos, "Matrix Theory Of Phtoelasticity",
Spriger-Verlag, 1979.

[9] G.B.Hocker,"Fiber Optic Sensing of Pressure and Temperature",
Applied Optics, vol. 18, No. 9, !st may 1979.

[10] Yasuharu Suematsu, "Introduction to Optical Fiber Communications",
JW&S, 1982.

[11] Namihira, et al., "Effect of Mechanical stress on the Transmission
Characteristics of Optical Fiber", Electronics and Communications in
Japan, V0l. 60-C, No. 7, 1977.

[12] L.B.Jeunhomme, "Single Mode Fiber Optics", Marcel Dekker Inc., 1983.

VITA

K. T. Srinivas was born on 4th March, 1961 in Bangalore India. He attended the National High School at Bangalore. He obtained his Bachelor of Engineering degree in Electronics from the Bangalore University in the year 1984. He received his Masters degree in Electrical Engineering in January 1987 from Virginia Polytechnic Institute & State University.

He has co-authored one technical paper. He is a member of the IEEE and the Communications Society. He is an amateur radio enthusiast.